Proc. 8th Int. Conf. Quarks and Nuclear Physics (QNP2018)
JPS Conf. Proc. **26**, 023001 (2019)
https://doi.org/10.7566/JPSCP.26.023001

η Photoproduction off the Deuteron and Low-Energy η-Nucleon Interaction

Satoshi X. Nakamura[1], Hiroyuki Kamano[2], and Takatsugu Ishikawa[3]

[1]*Laboratório de Física Teórica e Computacional - LFTC, Universidade Cruzeiro do Sul, São Paulo, SP 01506-000, Brazil*
[2]*Research Center for Nuclear Physics, Osaka University, Ibaraki, Osaka 567-0047, Japan*
[3]*Research Center for Electron Photon Science (ELPH), Tohoku University, Sendai, Miyagi 982-0826, Japan*

E-mail: sxnakamura@gmail.com

(Received December 14, 2018)

We study η photoproduction off the deuteron ($\gamma d \to \eta pn$) at a special kinematics: $\sim$ 0.94 GeV of the photon beam energy and $\sim 0^\circ$ of the scattering angle of the proton. This kinematics is ideal to extract the low-energy η-nucleon scattering parameters such as $a_{\eta N}$ (scattering length) and $r_{\eta N}$ (effective range) because the η-nucleon elastic scattering is significantly enhanced. We show that if a ratio R, the $\gamma d \to \eta pn$ cross section divided by the $\gamma p \to \eta p$ cross section convoluted with the proton momentum distribution in the deuteron, is measured with 5% error, Re[$a_{\eta N}$] (Re[$r_{\eta N}$]) can be determined at the precision of $\sim \pm 0.1$ fm ($\sim \pm 0.5$ fm), significantly narrowing down the currently estimated range of the parameters. The measurement is ongoing at the Research Center for Electron Photon Science (ELPH), Tohoku University.

KEYWORDS: meson photoproduction, hadron-hadron interaction, η-mesic nuclei

1. Introduction

The low-energy η-nucleon interaction can be characterized with two parameters, the scattering length $a_{\eta N}$ and effective range $r_{\eta N}$. The existence of exotic η-mesic nuclei largely depends on $a_{\eta N}$ that determines the attractive or repulsive nature of the low-energy ηN interaction [1]. However, $a_{\eta N}$ has not been well determined yet. Previous works have attempted to extract $a_{\eta N}$ and $r_{\eta N}$ by analyzing the $\pi N \to \pi N, \eta N$ and $\gamma N \to \pi N, \eta N$ reaction data [1], and also the $pn \to \eta d$ reaction data [2]. These analyses gave fairly consistent results for the imaginary parts of $a_{\eta N}$ and $r_{\eta N}$ which are within Im[$a_{\eta N}$] = 0.2–0.3 fm and Im[$r_{\eta N}$] = −1–0 fm, respectively [1]. However, their real parts are not well-determined: Re[$a_{\eta N}$] = 0.2–0.9 fm and Re[$r_{\eta N}$] = −6 to +1 fm. The large model-dependence in the real parts stems from the difficulty of isolating the ηN scattering amplitudes from other mechanisms involved in the reactions analyzed.

An ongoing η photoproduction experiment [3] at the Research Center for Electron Photon Science (ELPH), Tohoku University is designed to overcome the difficulty of determining $a_{\eta N}$ by utilizing a special kinematics. In this experiment, a photon beam with $E_\gamma \sim 0.94$ GeV hits a deuteron target and the recoil proton from $\gamma d \to \eta pn$ is detected at $\theta_p \sim 0^\circ$. At this kinematics, an η produced from a quasi-free proton is almost at rest, and thus it would interact strongly with the spectator neutron. On the other hand, the struck proton goes away with a large momentum, and thus it would not interact with the η and neutron. This seems an ideal kinematical condition, referred to as the ELPH kinematics, to determine the low-energy ηN scattering parameters. The present theoretical analysis [4] will show that a combined cross-section data for $\gamma d \to \eta pn$ and $\gamma p \to \eta p$ expected to be taken in the ELPH experiment would indeed lead to significant reduction of the current uncertainty of $a_{\eta N}$ and $r_{\eta N}$.

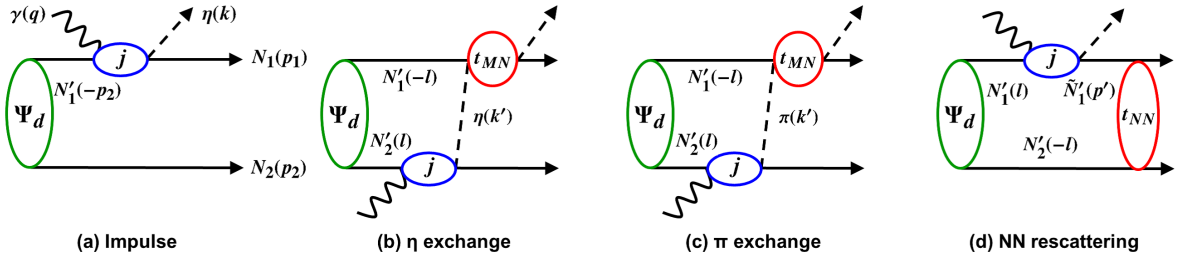

Fig. 1. Reaction mechanisms for $\gamma d \to \eta N_1 N_2$: (a) impulse, (b) η-exchange, (c) π-exchange, and (d) NN rescattering mechanisms. The figure taken from Ref. [4]. Copyright (2017) APS

2. Model

We study $\gamma d \to \eta pn$ relevant to the ELPH experiment with a model based on the impulse and the first-order rescattering mechanisms as illustrated in Fig. 1. The η-exchange mechanism [Fig. 1(b)] contains the $\eta N \to \eta N$ subprocess we are interested in, while the other mechanisms (the impulse [Fig. 1(a)], π-exchange [Fig. 1(c)], and NN-rescattering [Fig. 1(d)] mechanisms) are background processes. The model must be built with reliable amplitudes for elementary $\gamma N \to MN$, $MN \to M'N$, and $NN \to NN$ processes with $M^{(\prime)}$=π, η, as well as with a realistic deuteron wave function. By doing so, we can reliably isolate the amplitude for the $\eta N \to \eta N$ subprocess from data using well-predicted background contributions. Regarding $\gamma N \to MN$ and $MN \to M'N$ amplitudes, we employ those generated with a dynamical coupled-channels (DCC) model [5,6]. The DCC model is a multichannel unitary model for the πN and γN reactions in the nucleon resonance region. It was constructed fitting $\sim 27,000$ data points, and successfully describes [5, 6] $\pi N \to \pi N, \pi\pi N, \eta N, K\Lambda, K\Sigma$ and $\gamma N \to \pi N, \pi\pi N, \eta N, K\Lambda, K\Sigma$ reactions over the energy region from the thresholds up to $\sqrt{s} \lesssim 2.1$ GeV. For example, the DCC model describes $\gamma p \to \eta p$ differential cross sections in a very good agreement with data over the energy region relevant to the following calculations of $\gamma d \to \eta pn$. This confirms that the most important $\gamma p \to \eta p$ amplitudes among the elementary amplitudes for describing $\gamma d \to \eta pn$ have been well tested by the data. This DCC model predicts the ηN scattering parameters to be $a_{\eta N} = 0.75 + 0.26i$ fm and $r_{\eta N} = -1.6 - 0.6i$ fm, which are consistent with the previously estimated ranges. As for the deuteron wave function and the NN scattering amplitudes, we use the CD-Bonn potential [7] to generate them.

3. Result

We can make a parameter-free prediction for the $\gamma d \to \eta pn$ cross sections using the model described above. We can thus assess the validity of the model by confronting our model predictions with existing data. In Fig. 2(left), we show $d\sigma/d\Omega_\eta$ at $E_\gamma = 775$ MeV from our DCC-based model with and without the rescattering contributions along with the data. Our parameter-free prediction is found to be in an excellent agreement with the data. The $\eta N \to \eta N$ rescattering gives a slight enhancement in the backward direction, which is important for this nice agreement. A similar DCC-based model for $\gamma d \to \pi NN$ [9,10] also gives predictions that agree well with data by taking account of significant rescattering effects.

We now move on to the $\gamma d \to \eta pn$ reaction at the ELPH kinematics ($E_\gamma = 0.94$ GeV and $\theta_p = 0^\circ$). In Fig. 2(right-top), the predicted threefold differential cross section, $d^3\sigma/dM_{\eta n}d\Omega_p$, are presented as a function of the η-neutron invariant mass $M_{\eta n}$. The impulse mechanism [Fig. 1(a)] including the $\gamma p \to \eta p$ ($\gamma n \to \eta n$) amplitudes gives the dominant (negligible) contribution. A substantial contribution is from the η-exchange mechanism [Fig. 1(b)], and the cross sections including the impulse mechanisms only are changed by −40 to +20% [difference between the dashed and dotted

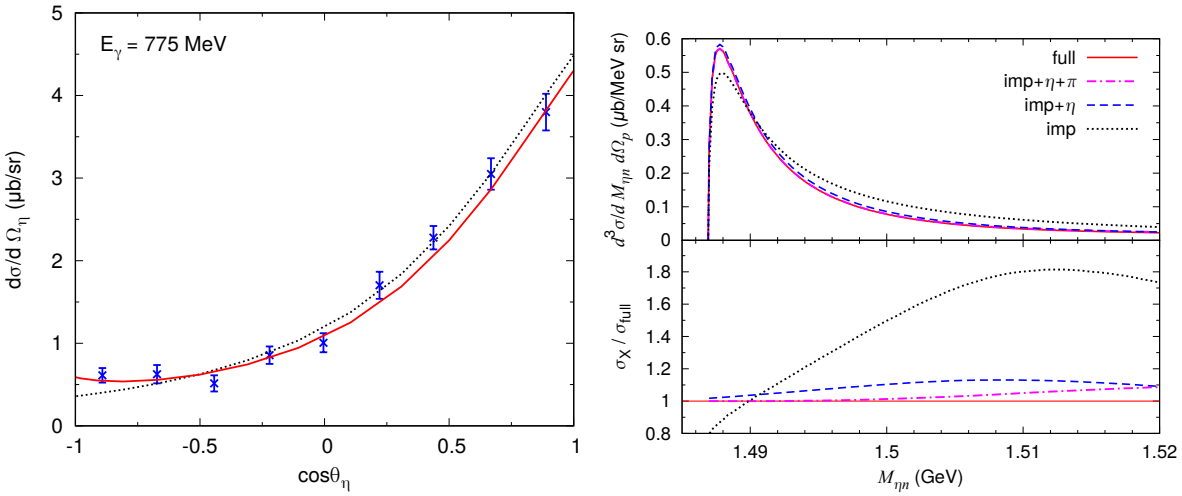

Fig. 2. [Left] Predicted differential cross sections for $\gamma d \to \eta pn$. The dotted curve is from the impulse approximation, and the solid curve includes rescattering mechanisms in addition. The data are from Ref. [8]. [Right-Top] Differential cross section for $\gamma d \to \eta pn$ at $E_\gamma = 0.94$ GeV and $\theta_p = 0°$. The impulse approximation (dotted curve), the impulse and η-exchange mechanisms (dashed curve), the impulse, η- and π-exchange mechanisms (dash-dotted curve), and the full calculation (solid curve). [Right-Bottom] Ratios of the differential cross sections from the various sets of the mechanisms to those from the full calculation. The figures taken from Ref. [4]. Copyright (2017) APS

curves in Fig. 2(right-bottom)]. The π-exchange [Fig. 1(c)] contribution is smaller, suppressing the cross sections by $\lesssim 9\%$ (difference between the dashed and dash-dotted curves). The NN rescattering [Fig. 1(d)] contribution (deviation of the dash-dotted curve from 1) is very small for $M_{\eta n} \lesssim 1.5$ GeV. This feature is what we expect to find in this special kinematics, and indicates that the proton essentially does not interact with the ηn system. Thus multiple rescatterings beyond the first-order rescattering [Figs. 1(b)–1(d)] should be safely neglected for $M_{\eta n} \lesssim 1.5$ GeV. We have also examined an off-shell momentum effect associated with the $\eta n \to \eta n$ scattering amplitude and found it very small. Because we are interested in a $M_{\eta n}$ region close to the threshold, higher partial waves for the $\eta n \to \eta n$ amplitudes are negligible. Therefore, we modify the full $\gamma d \to \eta pn$ model by replacing the ηn scattering amplitude with the S-wave one parametrized with $a_{\eta N}$ and $r_{\eta N}$. These scattering parameters are determined by analyzing the forthcoming ELPH data.

The ELPH data will be given in a form of the ratio, denoted by $R_{\rm expt}$, of the measured cross sections for $\gamma d \to \eta pn$ divided by those for $\gamma p \to \eta p$ convoluted with the proton momentum distribution in the deuteron. This is for removing systematic uncertainties of the acceptance from the detector coverage. Therefore, from the theoretical side, we need to calculate the corresponding quantity given by

$$R_{\rm th}(M_{\eta n}) = \frac{d^3\sigma_{\rm full}/dM_{\eta n}d\Omega_p|_{\theta_p=0°}}{d^3\sigma_{\rm imp}/dM_{\eta n}d\Omega_p|_{\theta_p=0°}}\,, \tag{1}$$

where $\sigma_{\rm full}$ ($\sigma_{\rm imp}$) is calculated with the full model (the impulse term only). Now the question is how sensitive $R_{\rm th}$ is against changing $a_{\eta N}$ and $r_{\eta N}$. Also, we are interested in what is the required precision of $R_{\rm expt}$ for significantly reducing the current uncertainties of $a_{\eta N}$ and $r_{\eta N}$.

First Re$[a_{\eta N}]$ is changed over 0.2 – 1.0 fm, with Im$[a_{\eta N}] = 0.25$ fm and $r_{\eta N} = 0$ fm being fixed. The resulting cross sections cover the red striped region as shown in Fig. 3(top), within the considered ELPH kinematics and $M_{\eta n} \leq 1.505$ GeV. The ratio $R_{\rm th}$ also changes accordingly as shown in Fig. 3(bottom); $R_{\rm th}$ shows more clearly the sensitivity to the variation of Re$[a_{\eta N}]$. The cross section and thus $R_{\rm th}$ changes by ~25% at the quasi-free (QF) peak position of $M_{\eta n} \sim 1.488$ GeV, as indicated

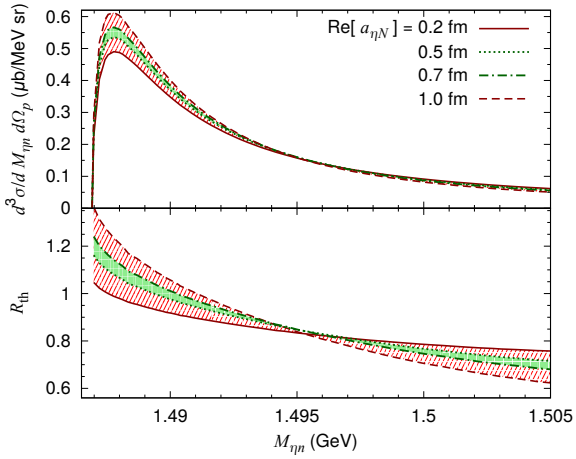

Fig. 3. (Top) Re[$a_{\eta n}$]-dependence of $\gamma d \to \eta pn$ differential cross sections from the full model; E_γ = 0.94 GeV and $\theta_p = 0°$. The curves correspond to Re[$a_{\eta n}$] = 0.2, 0.5, 0.7, and 1.0 fm; Im[$a_{\eta n}$] = 0.25 fm and $r_{\eta n}$ = 0. (Bottom) The ratio $R_{\rm th}$ given by Eq. (1) calculated with different values of Re[$a_{\eta n}$]. Figure taken from Ref. [4]. Copyright (2017) APS

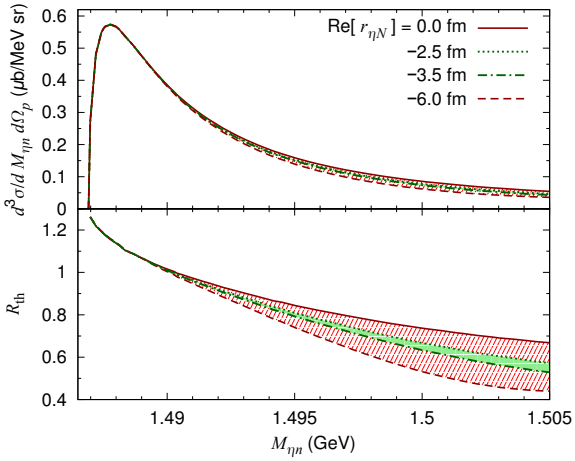

Fig. 4. Presentation similar to Fig. 3, but obtained with Re[$r_{\eta n}$] = 0 fm (solid), −2.5 fm (dotted), −3.5 fm (dash-dotted), and −6 fm (dashed); $a_{\eta n}$ = 0.75 + 0.26i fm and Im[$r_{\eta n}$] = 0 fm. The figure taken from Ref. [4]. Copyright (2017) APS

by the width of the striped band. We also show the green solid bands that have the widths of ∼5% at the QF peak. This green band is covered by our model when Re[$a_{\eta N}$] is varied by ±0.1 fm from 0.6 fm. This means that $R_{\rm expt}$ data of 5% error per MeV bin can determine Re[$a_{\eta N}$] at the precision of ∼ ±0.1 fm, significantly reducing the currently estimated range. Data of $R_{\rm expt}$ with this precision is expected to be taken in the ongoing ELPH experiment [3].

Next Re[$r_{\eta N}$] is varied over −6 – 0 fm which is the currently estimated range, while the scattering length being fixed at the value from the latest DCC analysis [6], $a_{\eta n}$ = 0.75+0.26i fm; Im[$r_{\eta N}$] = 0 fm. Accordingly, the cross section and $R_{\rm th}$ change over the red striped region in Fig. 4. The effect of changing $r_{\eta N}$ is visible at ∼5 MeV above the ηN threshold. The ratio $R_{\rm th}$ at $M_{\eta n}$ = 1.5 GeV changes by ∼30% (∼5%) when Re[$r_{\eta N}$] is changed over −6 – 0 fm (−3.5 to −2.5 fm) as indicated by the red striped (green solid) band. Therefore, Re[$r_{\eta N}$] at the precision of $\lesssim$ ±0.5 fm, which is significantly improved precision over the current estimates, can be obtained by measuring $R_{\rm expt}$ data of 5% error per MeV bin.

Acknowledgments

This work is in part supported by Fundação de Amparo à Pesquisa do Estado de São Paulo (FAPESP), Process No. 2016/15618-8, and by JSPS KAKENHI Grant Number JP18K03632.

References

[1] Q. Haider and L. C. Liu: Int. J. Mod. Phys. E **24** (2015) 1530009
[2] H. Garcilazo and M. T. Peña: Eur. Phys. J. A **38** (2008) 209
[3] T. Ishikawa *et al.*: JPS Conf. Proc. **13** (2017) 020031; Acta Phys. Polon B **48** (2017) 1801
[4] S.X. Nakamura, H. Kamano, T. Ishikawa: Phys. Rev. C **96** (2017) 042201(R)
[5] H. Kamano, S.X. Nakamura, T.-S.H. Lee, T. Sato: Phys. Rev. C **88** (2013) 035209
[6] H. Kamano, S.X. Nakamura, T.-S.H. Lee, T. Sato: Phys. Rev. C **94** (2016) 015201
[7] R. Machleidt: Phys. Rev. C **63** (2001) 024001
[8] B. Krusche *et al.*: Phys. Lett. B **358** (1995) 40
[9] S.X. Nakamura, H. Kamano, T.S.H. Lee, T. Sato: arXiv:1804.04757
[10] S.X. Nakamura: Phys.Rev. C **98** (2018) 042201(R)